Redox Biology 15 (2018) 170–181

Contents lists available at ScienceDirect

Redox Biology

journal homepage: www.elsevier.com/locate/redox

Short-term sustained hyperglycaemia fosters an archetypal senescence-associated secretory phenotype in endothelial cells and macrophages

Francesco Prattichizzo[a,b,*], Valeria De Nigris[b,c], Elettra Mancuso[b,d], Rosangela Spiga[b,d], Angelica Giuliani[e], Giulia Matacchione[e], Raffaella Lazzarini[f], Fiorella Marcheselli[g], Rina Recchioni[g], Roberto Testa[h], Lucia La Sala[a], Maria Rita Rippo[e], Antonio Domenico Procopio[e,g], Fabiola Olivieri[e,g], Antonio Ceriello[b,c,i]

[a] IRCCS MultiMedica, Sesto San Giovanni,Milano, Italy
[b] Diabetes and Obesity Research Laboratory, Institut d'Investigacions Biomèdiques August Pi I Sunyer (IDIBAPS), Barcelona, Spain
[c] CIBER de Diabetes y Enfermedades Metabólicas Asociadas (CIBERDEM), Spain
[d] Department of Medical and Surgical Sciences, Viale Europa, University Magna-Græcia of Catanzaro, Italy
[e] Department of Clinical and Molecular Sciences, DISCLIMO, Università Politecnica delle Marche, Ancona, Italy
[f] Department of Molecular and Clinical Sciences - Histology, Marche Polytechnic University, Ancona, Italy
[g] Center of Clinical Pathology and Innovative Therapy, INRCA-IRCCS National Institute, Ancona, Italy
[h] Clinical Laboratory and Molecular Diagnostics, INRCA-IRCCS National Institute, Ancona, Italy
[i] Department of Cardiovascular and Metabolic Diseases, IRCCS Multimedica, Sesto San Giovanni, Milano, Italy

ARTICLE INFO

Keywords:
Diabetes
Senescence associated secretory phenotype
Endothelial cells
Macrophages
Inflammation
Anion superoxide

ABSTRACT

Diabetic status is characterized by chronic low-grade inflammation and an increased burden of senescent cells. Recently, the senescence-associated secretory phenotype (SASP) has been suggested as a possible source of inflammatory factors in obesity-induced type 2 diabetes. However, while senescence is a known consequence of hyperglycaemia, evidences of SASP as a result of the glycaemic insult are missing. In addition, few data are available regarding which cell types are the main SASP-spreading cells *in vivo*.

Adopting a four-pronged approach we demonstrated that: i) an archetypal SASP response that was at least partly attributable to endothelial cells and macrophages is induced in mouse kidney after *in vivo* exposure to sustained hyperglycaemia; ii) reproducing a similar condition *in vitro* in endothelial cells and macrophages, hyperglycaemic stimulus largely phenocopies the SASP acquired during replicative senescence; iii) in endothelial cells, hyperglycaemia-induced senescence and SASP could be prevented by SOD-1 overexpression; and iiii) *ex vivo* circulating angiogenic cells derived from peripheral blood mononuclear cells from diabetic patients displayed features consistent with the SASP.

Overall, the present findings document a direct link between hyperglycaemia and the SASP in endothelial cells and macrophages, making the SASP a highly likely contributor to the fuelling of low-grade inflammation in diabetes.

1. Introduction

Type 2 diabetes, obesity, and metabolic syndrome are associated with an increased inflammatory score [1,2]. The term 'metaflammation' was coined some years ago to indicate metabolically triggered inflammation [2]. The condition, which is mainly fostered by nutrient and metabolic surplus, is characterized by a set of molecules and signalling pathways similar to those involved in classic inflammation [2]. Recently, the senescence-associated secretory phenotype (SASP) has been suggested to be a major contributor to metaflammation in obesity as well as in type 2 diabetes [3–8]. The SASP consists of a transcriptional pro-inflammatory program that is activated following senescence growth arrest and involves the secretion of a variety of molecules including cytokines, chemokines, and growth factors [9]. In mouse models, removal of senescent cells (SCs) induced an increase in lifespan and healthspan and reduced inflammation in various organs, including kidney [10]. These findings suggest that the SASP plays a major role in inflammaging, the chronic, low-grade inflammatory state that accompanies aging [10,11]. There is substantial evidence that the SASP is an early event preceding insulin sensitivity loss in adipose tissue of obese

* Corresponding author at: Department of Cardiovascular Research, IRCCS MultiMedica, Milano, Italy.
E-mail address: f.prattichizzo@univpm.it (F. Prattichizzo).

https://doi.org/10.1016/j.redox.2017.12.001
Received 14 September 2017; Received in revised form 30 October 2017; Accepted 4 December 2017
Available online 06 December 2017

mice and humans [6,12,13]. Moreover, in aged mice SASP inhibition improved glycaemic parameters by increasing insulin sensitivity [14]. Hyperglycaemia (HG) is known to induce senescence *in vitro* [15], but *in vivo* evidence of accelerated senescence in diabetic mice and humans has also been provided [15–17]. These data suggested the existence of a feedback loop between type 2 diabetes and the SASP [3,4]. However, there is no evidence that HG is a direct cause of SASP acquisition *in vivo*. It is also unclear whether it can trigger a secretory profile comparable to the one induced by classic pro-senescence stimuli, *e.g.* replicative exhaustion [4]. Moreover, little is known regarding which cell types are the main SASP-spreading cells *in vivo* [18,19]. In this study, a mouse model of short-term sustained HG was used to investigate senescence and inflammation in kidney, a prototypical organ damaged by diabetes. Moreover, since *in vivo* data suggest that endothelial cells (ECs) and macrophages are key SASP-carrying cells, human cell lines were used to dissect the secretome/phenotype induced by HG in these cell types *in vitro*. Finally, circulating angiogenic cells (CACs) isolated from healthy subjects and age-matched diabetic patients were studied *ex vivo* to gain preliminary insights into the significance of these phenomena in humans.

2. Materials and methods

2.1. STZ treatment and tissue sampling

Male C57BL/6 mice kept in a standard light/dark cycle (12 :12 h) with free access to standard chow and water were studied at the age of 25 weeks. Diabetes was induced by a single intraperitoneal injection (150 mg kg − 1) of STZ in 0.05 M citrate buffer (pH 4.5) vehicle. Animals were fasted for 4 h before and 30 min after the injection. Control mice received the vehicle alone. No acute tubular cytotoxicity was detected [20] (Fig. 1B). All STZ-treated mice developed sustained HG but experienced no episode of severe hyperglycaemia (blood glucose > 600 mg/dl) (Supplementary Table 1). Animals were not randomized to the experiments. Twelve mice were used for each experimental condition. All animals were included in data analysis. Sample size was selected on the basis of previous publications [7,12,14] and it was not calculated by statistics. Mice were sacrificed 7 days after STZ injection. Kidneys were immediately extracted and snap-frozen for RNA and protein analysis, fixed overnight in 4% paraformaldehyde (Sigma-Aldrich) for immunohistochemistry, or stained directly for SA β-gal. *In vivo* studies were performed with approval of the University of Barcelona Ethics Committee, complying with current Spanish and European legislation.

2.2. SA β-gal analysis

Freshly isolated kidneys were cut into 4 portions to maximize penetration. After 5 min fixation and overnight staining with Cellular Senescence Assay Kit solutions (CBA 230, Cell Biolabs), 2 portions were included in paraffin and sections 5 μm in thickness were cut, stained with Nuclear Fast Red (Sigma-Aldrich), and subjected to histological examination. The remaining 2 portions of each kidney were weighed and homogenized in an equal volume of PBS and the solutions were read with a spectrophotometer at OD 595. A fluorescence-based protocol [19] was used to assess SA β-gal activity in protein lysates from kidney and cell-derived samples.

2.3. Immunohistochemistry

Nine non-consecutive sections (5 μm thick) of each kidney portion were mounted on microscope slides. Prior to immunohistochemical staining, sections were deparaffinized, rehydrated, permeabilized, processed for antigen retrieval, and blocked in 3% BSA. Primary antibody used p16 (C-7: sc-377412; Santa Cruz) was dissolved in PBS 1X/ 0.1 BSA buffer and stined overnight at 4oC). Alexa Fluor 555–donkey anti-mouse IgG (A-31570) was used as secondary antibodies and negative control. Slides were mounted with Dako fluorescent mounting medium. Images were acquired with a Leica TCS SPE confocal microscope.

2.4. Macrophages and endothelial cells isolation from kidneys

Mice kidneys were digested with Multi Tissue Dissociation Kit 2 (Miltenyi Biotec) to form a cell suspension. Then, F4/80 positive macrophages were sorted with Anti-F4/80 MicroBeads UltraPure (Miltenyi Biotec) according to manufacturer instructions for manual separation. Negatively selected cells were further sorted to collect endothelial cells with CD31 MicroBeads (Miltenyi Biotec). Negatively selected cells were collected as well and the three cell populations were directly subjected to mRNA extraction, cDNA synthesis and RT–PCR analysis.

2.5. Cell cultures

HUVECs from three batches (1 from single donor and 2 from pooled donors) were cultured in EGM-2 endothelial growth medium (Lonza). Replicative senescence was studied by culturing cells up to the 15/16th or the 20th passage, depending on the batch. CPD was calculated as the sum of all population doubling (PD) changes. Cells were divided into young (SA β-gal < 10%) and senescent (SA β-gal > 50%).

Human THP-1 and U937 cells were purchased from ATCC and maintained in RPMI-1640 medium supplemented with 10% FBS, 1% penicillin/streptomycin, and 1% L-glutamine (Euroclone). A published protocol [34] was used for macrophages derived from THP-1 and U937 cells. The proportion of SA β-gal+ cells was assessed as described previously [21,50].

2.6. Total RNA extraction

Total RNA was purified using an RNA purification kit (Norgen Biotek) according to the manufacturer's instructions.

2.7. RT qPCR for mRNA expression

Total RNA (1–2 μg) was reverse-transcribed with Superscript III RT kit according to the manufacturer's instructions. Real-time PCR (RT-PCR) was performed in an ABI Prism 7900 sequence detection system using SybrGreen reagents (Takara Bio Company) and TaqMan® Gene Expression Master Mix (Life Technologies). Values were normalized to GAPDH RNA levels for human cells and mouse kidney. Bcl-2, p21 and p53 were analysed with the TaqMan Gene Expression assay (Applied Biosystems). Thermal profiles used were previously published [51,52]. The primers for all the other mRNAs are listed in Table 4 of supplemental material.

2.8. MiRNA quantification by RT qPCR

MiRNA expression was quantified using a modified real-time approach using TaqMan MicroRNA RT kit and a miRNA assay (both from Applied Biosystems). Procedures and thermal profiles were previously published [50]. MiRs expression in HUVECs was evaluated using RNU44 as the reference; for miRs expression in kidneys RNU 6b was used as the reference.

2.9. Senescence mRNA profiling

Three different HUVEC batches were exposed to hyperglycaemic medium for a week, subcultured until the onset of replicative senescence (> 50 PD and SA β-gal positivity > 50%), or left untreated (control). Total RNA from treated cells was isolated using Master Script RT-PCR System (5 PRIME). cDNA synthesis was performed using SA

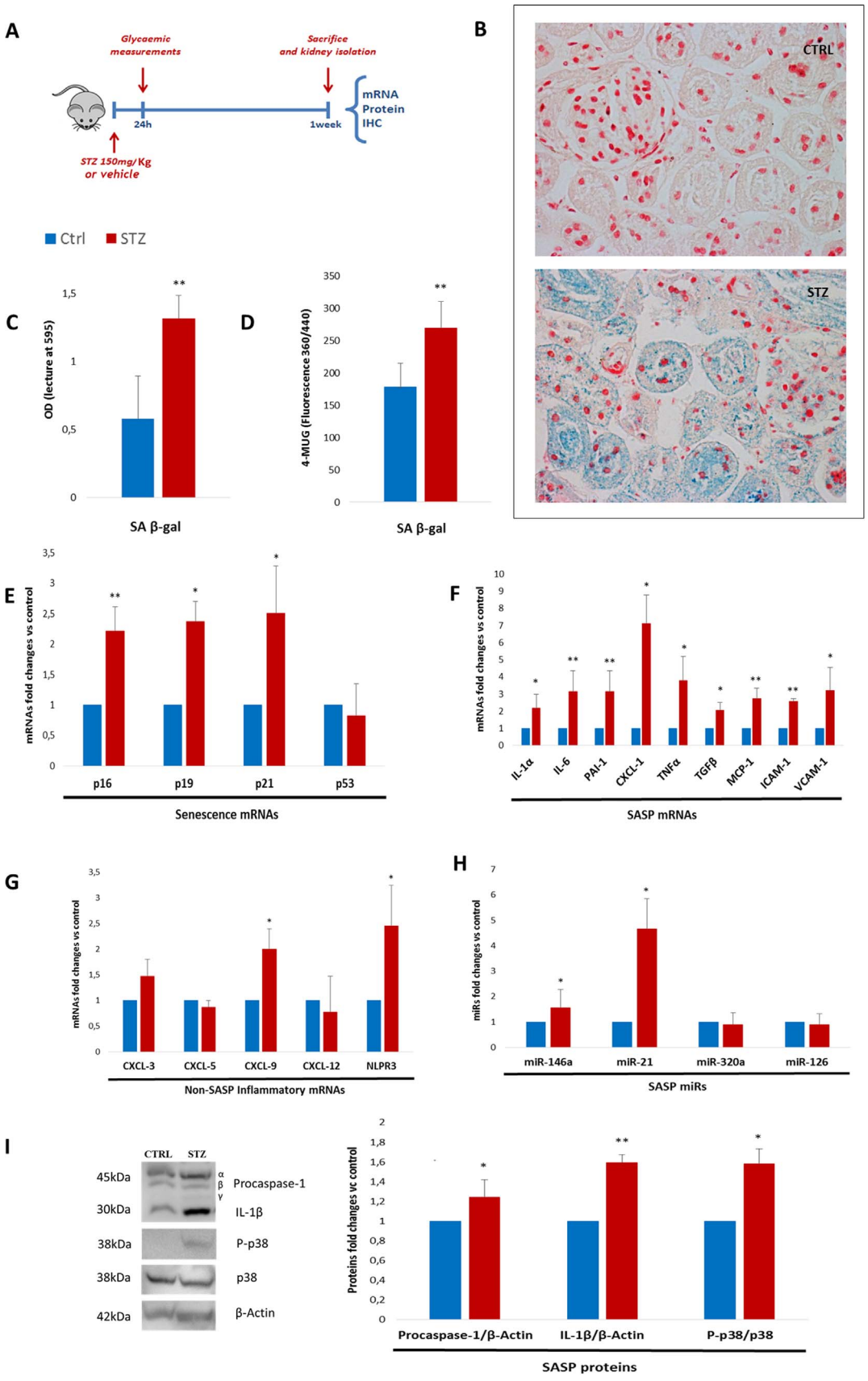

(caption on next page)

Fig. 1. One-week hyperglycaemia induces senescence and SASP acquisition in kidneys of STZ diabetic mice A. Experimental design (12 mice/group). B. Representative SA β-gal staining (nuclei stained with Fast Red, 20x magnifications) and measurement of blue reaction product with OD reading of organ-derived homogenate, normalized to sample weight (3 mice/group). C. SA β-gal activity measured in protein lysates, normalized to protein content (3 mice/group). D. Fold changes in expression levels of SA mRNAs (*p16, p19, p21*, and *p53*) (4 mice/group) E. Fold changes in expression levels of SASP mRNAs (*IL-1α, IL-6, PAI-1, CXCL-1, TNF-α, TGF-β, MCP-1, ICAM-1*, and *VCAM-1*) (4 mice/group) F. Fold changes in expression levels of non-SASP inflammatory mRNAs (*CXCL-3, CXL-5, CXCL-9, CXCL-12,* and *NPLR3*) (4 mice/group) G. Fold changes in SASP-related microRNAs (*miR-146a*, *miR-21, miR-320a*, and *miR-126*) (4 mice/group). H. Western blot assessment of SASP proteins (caspase-1, IL-1β, and p-p38) (3 mice/group). Blue histograms = means of vehicle-treated mice (Ctrl); red histograms = means of STZ-treated hyperglycaemic mice (HG-M). For all diagrams error bars are ± SD and * *t*-test $p < 0.05$, ** *t*-test $p < 0.01$.

Biosciences RT^2 First Strand Kits. Cellular Senescence RT2 Profiler PCR Array (PAHS-050ZA Qiagen) was used. The average of hypoxanthine phosphoribosyltransferase 1 (HPRT1) and ribosomal protein, large, P0 (RPLP0) was used for normalization. Only mRNAs with reads < 35 Ct in all three biological replicates were included in the analysis. Averages of the relative expression (2-ΔCt) of HUVECs exposed to HG or cultured until replicative senescence were compared with control cells to calculate fold changes. Only genes where differences reached a p level < 0.05 are presented. The dataset is available at GEO repository under accession number GSE99013.

2.10. Protein extraction and immunoblotting

Cells and kidney samples were lysed in RIPA buffer adding 10% proteases and 1% phosphatase inhibitors (Sigma-Aldrich). Protein concentration was determined using the Bradford assay (Sigma-Aldrich). For western blot analysis, 50 μg of lysate was separated by electrophoresis using PAGE gels (4–20%) (Cultek) and transferred to PVDF membranes (GE Healthcare). After blocking with 5% non-fat dried milk, membranes were incubated overnight at 4 °C with the following primary antibodies: anti-caspase-1 (#2225; Cell Signalling Technology), anti-IL-1β (ab9722; Abcam), anti-phospho-p38 Thr180/Tyr182 (#9211), anti-p38 tot (#9212), anti-p-NF-kB, anti-p21 (#2947; all from CST), anti-p15/16, anti-IL-8 (ab110727; Abcam), anti-SOD-1 (#2770; CST), anti-PKCβ (sc-8049; Santa Cruz), and anti-β-actin (A2066; Sigma). Secondary IgG HP-conjugated anti-mouse or anti-rabbit (GE Healthcare) were applied for 1 h at room temperature. Immunoreactive proteins were revealed with Luminata Forte (Millipore) using LAS4000. When necessary, membranes were stripped with commercial stripping buffer solution (Thermo Scientific). β-actin was used as the loading control. Densitometric analysis was performed with Image J software.

2.11. ROS, O2-, and MDA dosage

ROS production and O2- were measured using the fluorescent probe 2',7'-dichlorofluorescein diacetate (H2DCFDA) and the Superoxide Anion Assay Kit (CS1000; Sigma). The latter method is based on the oxidation of luminol by superoxide anions resulting in the formation of chemiluminescence light. A specific enhancer amplifies the chemiluminescent signal. Fluorescence and chemiluminescence intensities were kinetically measured using a microplate reader (Synergy HT, BioTek Instruments). To estimate lipids peroxidation, the bi-product malondialdehyde (MDA) was dosed using a Lipid Peroxidation (MDA) Assay Kit (Abcam, ab118970), according to manufacturer instructions. Briefly, the MDA in the sample reacts with thiobarbituric acid (TBA) to generate a MDA-TBA adduct. The MDA-TBA adduct can be easily quantified colorimetrically (OD = 532 nm). Values were normalized for protein content of the lysates.

2.12. ELISA

Conditioned media (CM) were prepared by incubating cells for 18 h in serum-free medium after the end of treatments. Cells were counted for normalization purposes. After centrifugation, CM samples were stored at −20 °C until use. IL-6 was measured using high-sensitivity ELISA kit (Invitrogen), while IL-8 and MCP-1 with the multi-analyte ELISArray Handbook (Qiagen).

2.13. Adenoviral infection

HUVECs were plated in complete EGM-2 medium and infected with adenovirus Ad-SOD1 or with GFP adenovirus as control (Ad-null) (#1503 and #1060; Vector Biolabs) with a viral load of 10 multiplicity of infection (MOI). After 12 h, media were changed and the experimental treatments begun.

2.14. CACs isolation

CACs were isolated from 14 ml heparinized peripheral blood collected from 13 type 2 diabetic patients and 10 age-matched healthy subjects. All patients gave their informed consent before participating in the study, which was approved by the INRCA Institutional Ethical Board. PBMCs were isolated by density-gradient centrifugation with Ficoll (Ficoll-Paque™ PLUS) within 2 h of collection. 5×10^6 PBMCs were plated on 24-well fibronectin-coated plates (BD Biosciences) and maintained in endothelial basal medium (Lonza) supplemented with EGM SingleQuots and 20% foetal calf serum for 4 days. After 4 days in culture, non-adherent cells were removed by washing with PBS whereas adherent cells were lysed directly in the culture wells. The CAC phenotype was confirmed as described previously [37].

2.15. Statistical analysis

The experiments were not randomized and the investigators were not blinded during experiments. In vivo experiments were conducted on animals of the same age and gender, thus equal variance was assumed. Error bars are presented as mean ± standard deviation (SD). The significance of differences was determined using two-tailed Student's *t*-test. A level of $p < 0.05$ was considered significant. For each experiment, the number of replicates is indicated in the figure legends.

3. Results

3.1. One-week sustained hyperglycaemia induces SASP in mouse kidney

To investigate the ability of HG to induce SASP *in vivo*, mice were rendered hyperglycaemic by a single peritoneal injection of streptozotocin (STZ; 150 mg/kg). Non-fasting glycaemia was randomly measured on alternate days, beginning the next day, to confirm the state of sustained HG (> 300 < 600 mg/dl) (Supplementary Table 1). Seven days after the injection animals were sacrificed and the kidneys extracted and analysed (Fig. 1A). Selective β-cells toxicity was induced by a single moderate dose of STZ rather than using multiple low-dose injections, because they induce tissue damage through the adverse effects of oxidative stress and renal injury due to acute tubular cytotoxicity [20]. A short exposure time (one week) was selected to avoid the influence exerted by the development of diabetic nephropathy [20]. Staining of fresh tissue samples with senescence-associated (SA) β-gal, the most widely used senescence marker [21], demonstrated a significant increase in SA β-gal-positive (+) cells in hyperglycaemic mice (HG-M; Fig. 1B, C, D). Since control kidneys also showed occasional SA β-gal positivity (Fig. 1B), additional assays were applied to quantify the senescence burden. Stained kidneys were weighed and homogenized in phosphate-buffered saline (PBS) and homogenates were read with a spectrophotometer at an optical density (OD) of 595 (Fig. 1C). These results were confirmed in whole tissue protein lysates using a sensitive

fluorescence method [19] (Fig. 1D). Measurement of the mRNA expression levels of the major SA genes in whole kidney revealed a significant increase in *p16*, *p19*, and *p21* in HG-M (Fig. 1E). Dosage of a comprehensive panel of SASP factors [9] showed a significant increase of all tested mRNAs in kidney from HG-M compared with control animals (Fig. 1F), especially upstream cytokines controlling the SASP and downstream effectors, *i.e.* interleukin *(IL)−1α* and *IL-6* [22]. Interestingly, a number of inflammatory factors that are not part of the SASP [9] were not significantly different in the two groups of mice (Fig. 1G). Since senescence acquisition is accompanied by epigenetic rearrangements [23,24], microRNAs (miRNAs) related to SASP/senescence were also examined, to establish whether they were altered at such early time point after HG onset. *MiR-21* and *miR-146a* were significantly upregulated in kidney from HG-M (Fig. 1H), in line with previous reports [25,26]. Moreover, given that *NLPR3* mRNA expression was increased (Fig. 1G) and that the inflammasome platform controls paracrine transmission of senescence [27], caspase-1/IL-1β expression was evaluated by western blotting. Both full-length proteins were significantly higher in the protein lysates from HG-M kidneys, whereas the cleaved forms were undetectable (Fig. 1I). In addition, HG-M kidneys exhibited a significant increase in phosphorylation of p38 (Fig. 1I), the main kinase controlling SASP factor secretion [28].

3.2. Endothelial cells and macrophages are SASP-carrying cells in vivo

To substantiate expression data and identify possible candidate SCs *in vivo*, kidney sections were assessed for p16 staining. Positivity for p16 was absent or rare in control tissue, while kidneys of hyperglycaemic mice showed consistent positivity both around vessels/capillaries and within mesangium/glomeruli (Fig. 2A and data not shown). Thus, considering that previous literature suggest ECs and macrophages as possible SASP-carrying cells *in vivo* [8,16,18,19], we isolated F4/80+, F4/80-/CD31+, and F4/80-/CD31- cell populations and directly subjected them to senescence and SASP mRNA expression (Fig. 2B). Both macrophages and ECs displayed a signature compatible with the SASP (Fig. 2C). Interestingly, even non-endothelial, non-macrophagic cells showed increased expression of *p21* and *TGFβ* confirming that even kidney specific cell types can harbour a senescent and pro-inflammatory phenotype [39–41]. However, these data indicate that ECs and macrophages are SASP-carriers *in vivo* in HG-M kidneys.

3.3. SASPs induced by hyperglycaemia and by replicative exhaustion show a comparable transcriptional profile in endothelial cells

Since the *in vivo* data suggested that HG may induce ECs senescence, human umbilical vein endothelial cells (HUVECs) were subjected to comparative gene expression. Young ECs (cumulative population doubling [CPD] > 25, < 30; SA β-gal positivity < 10%) were exposed to hyperglycaemic medium (25 mmol/l) for a week or subcultured until complete growth arrest (CPD > 50). Array profiling showed a marked and largely overlapping pro-senescence response in HG-exposed and replicative senescent HUVECs (Fig. 3A). Real-time PCR analysis disclosed an elevation of the mRNA levels of the major SASP factors in both conditions (Fig. 3B and Supplementary Table 2). Interestingly, the increment in IL-10 and superoxide dismutase (SOD-1) transcripts following replicative exhaustion was not paralleled by an increase of these mRNAs in HG-induced SASP (Fig. 3A, B), suggesting an impaired anti-inflammatory and antioxidant compensatory response in ECs exposed to the hyperglycaemic environment. Both stimuli significantly increased SA β-gal positivity and activity (Fig. 3C). Dosage of the three main SASP products in the media of HG-exposed and replicative senescent HUVECs confirmed the mRNA results, since both insults resulted in significantly increased IL-6, IL-8, and monocyte chemoattractant protein (MCP)−1 release (Fig. 3D). Thus, since oxidative stress, particularly superoxide anion (O_2-), has been implicated as a major driver of both HG-induced EC dysfunction and endothelial senescence, the whole amount of reactive oxygen species (ROS) and O_2- were quantified. Both stimuli were associated with a dramatic increase in total ROS and O_2- levels (Fig. 3E, F), in line with evidence that oxidative stress is a major feature associated with hyperglycaemic injury and replicative senescence [29,30]. In addition, to quantify the burden of oxidative damage, we measured the levels of malondialdehyde (MDA), a common marker for lipids peroxidation. Both treatments induced a significant increase in MDA levels (Supplementary Fig. 1).

3.4. SOD-1 overexpression attenuates hyperglycaemia-induced senescence and the SASP in endothelial cells

Given the increased abundance of O_2- in HG-treated ECs and the absence of a compensatory increment of the detoxifying enzyme SOD-1, an adenoviral vector was used to induce SOD-1 overexpression prior to the hyperglycaemic insult. Measurement of its activity in ECs by real time PCR and western blot analysis demonstrated that the adenoviral vector was highly efficient also in the hyperglycaemic medium, and that forced SOD-1 expression was capable of reversing the HG-induced increase in protein kinase C beta (PKCβ), which is related to HG and O_2- [29,31] (Supplementary Fig. 2). Moreover, since a major SASP feature is the chronicity of the pro-inflammatory program [9], ECs exposed to one-week HG were switched to normoglycaemic medium for 3 days to measure hyperglycaemic memory (HM-ECs) (Fig. 4A). The increased SA β-gal activity induced by HG was maintained in HM-ECs and was significantly attenuated by SOD-1 overexpression, but not by the vector carrying GFP adenovirus (Ad-null) in control cells (Fig. 4B). The mRNA expression of the major SA genes, *i.e. p16*, *p21*, and the recently identified *Bcl-2* [32,33], followed the same trend, whereas *p53* expression was significantly increased only in HM-ECs (Fig. 4C). A large number of SASP mRNAs, *i.e. IL-1α*, *IL-6*, *IL-8*, tumour necrosis factor *(TNF)-α*, transforming growth factor *(TGF)-β*, plasminogen activator inhibitor *(PAI)−1*, *MCP-1*, intercellular adhesion molecule *(ICAM)−1*, vascular cell adhesion molecule *(VCAM)−1*, and insulin-like growth factor-binding protein (*IGFBP)6* were markedly increased in HG and HM-ECs, and their increase was partially but significantly attenuated by SOD-1 overexpression in both conditions (Fig. 4D). Western blot analysis confirmed the mRNAs results, since p16, p21, and IL-8 proteins showed a similar expression pattern (Fig. 4E). Moreover, expression of IL-1β and p38 and NF-kB phosphorylation were increased in HG-ECs and HM-ECs, an effect that was completely suppressed by SOD-1 overexpression (Fig. 4E). Dosage of the prototypical SASP protein IL-6 in the culture medium clearly reflected the drift towards the SASP induced by HG and its compensation by SOD-1 overexpression (Fig. 4F). Finally, upregulation of the SASP-associated *miR-146a* and *miR-21* was induced in HG-ECs and HM-ECs and was blunted in cells overexpressing SOD-1, whereas *miR-126* was downregulated in HG-ECs and HM-ECs (Fig. 4G), in line with previous findings [24].

3.5. Hyperglycaemia induces a SASP-like program in macrophages derived from THP-1 and U937 cells

Since the *in vivo* results suggested that macrophages may also be major SA cells, two human monocytic cell lines, THP-1 and U937, were differentiated *in vitro* and exposed for one week to hyperglycaemic (30 mmol/l) or normoglycaemic (10 mmol/l) medium and the resulting phenotype was evaluated. THP-1 cells were treated with low-dose PMA for 48 h to induce differentiation into macrophages without inducing a clear M1/M2 phenotype [34] and then exposed to hyperglycaemic medium. Strikingly, monocyte to macrophage differentiation induced the acquisition of SA β-gal positivity in a subset of cells and HG significantly strengthened this effect, since both SA β-gal activity and the number of SA β-gal+ cells (Fig. 5A, B) increased. Moreover, mRNA analysis revealed a clear SASP-like phenotype, since *IL-1α*, *IL-6*, *IL-8*, *PAI-1*, *TGF-β*, *TNF-α*, *MCP-1*, *ICAM-1*, and *IGFBP6* all showed marked

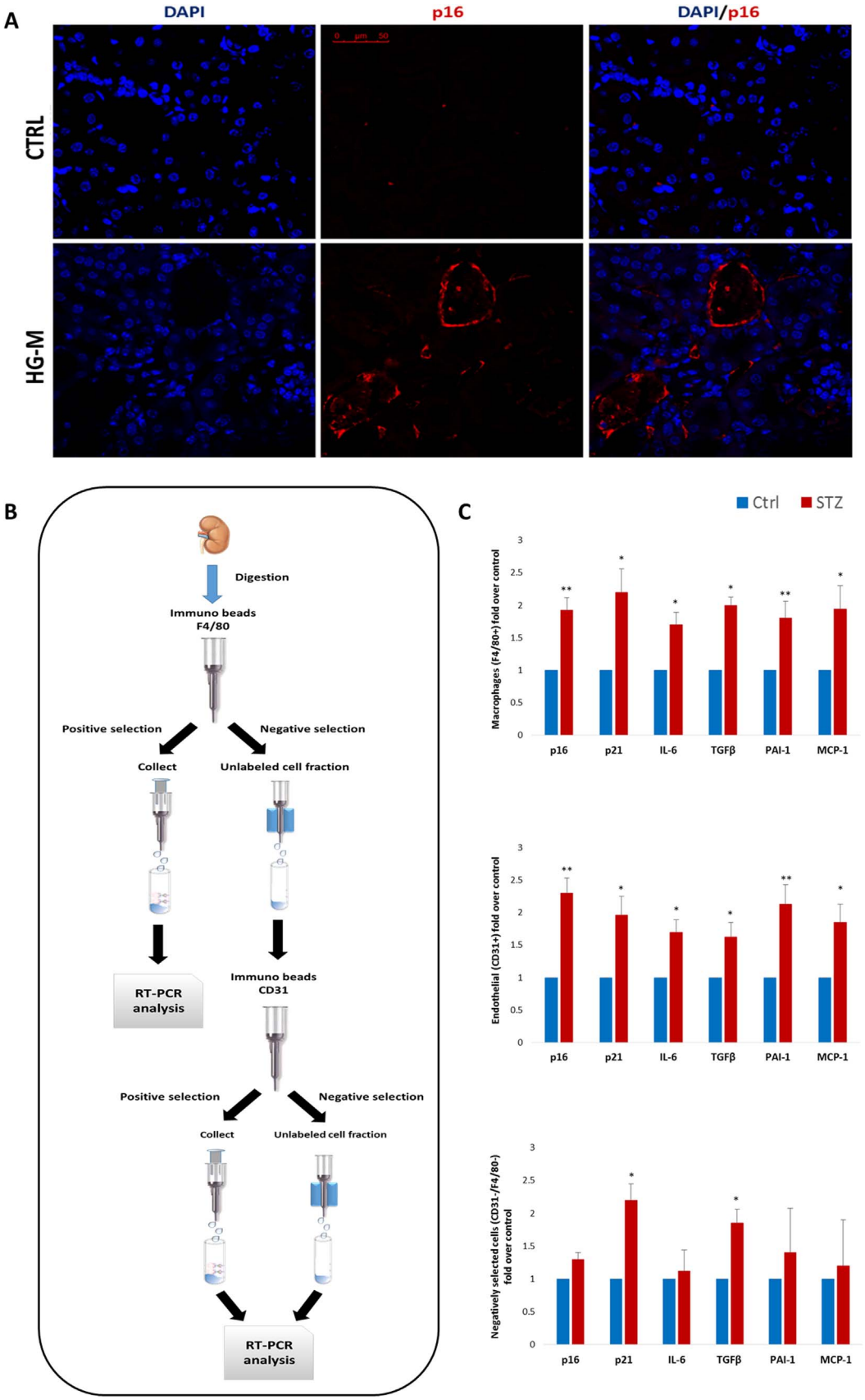

Fig. 2. Endothelial cells and macrophages are SASP-carrying cells in the diabetic mice kidney. A. Representative confocal microscope images of kidney sections stained for p16 (red) from control (Ctrl) and hyperglycaemic mice (HG-M). Nuclei are counterstained with DAPI (blue). Scale bar = 50 µm. B. Experimental design used to isolate macrophages, ECs, and non-macrophagic/non-endothelial cells from kidneys. C. Fold changes in sorted populations in expression levels of SA and SASP mRNAs (*p16, p21, IL-6, TGF-β, PAI-1* and *MCP-1*) (n = 3 mice/group). Blue histograms = means of vehicle-treated mice (Ctrl); red histograms = means of STZ-treated hyperglycaemic mice (HG-M). For all diagrams error bars are ± SD and * *t*-test $p < 0.05$, ** *t*-test $p < 0.01$ (For interpretation of the references to color in this figure legend, the reader is referred to the web version of this article.).

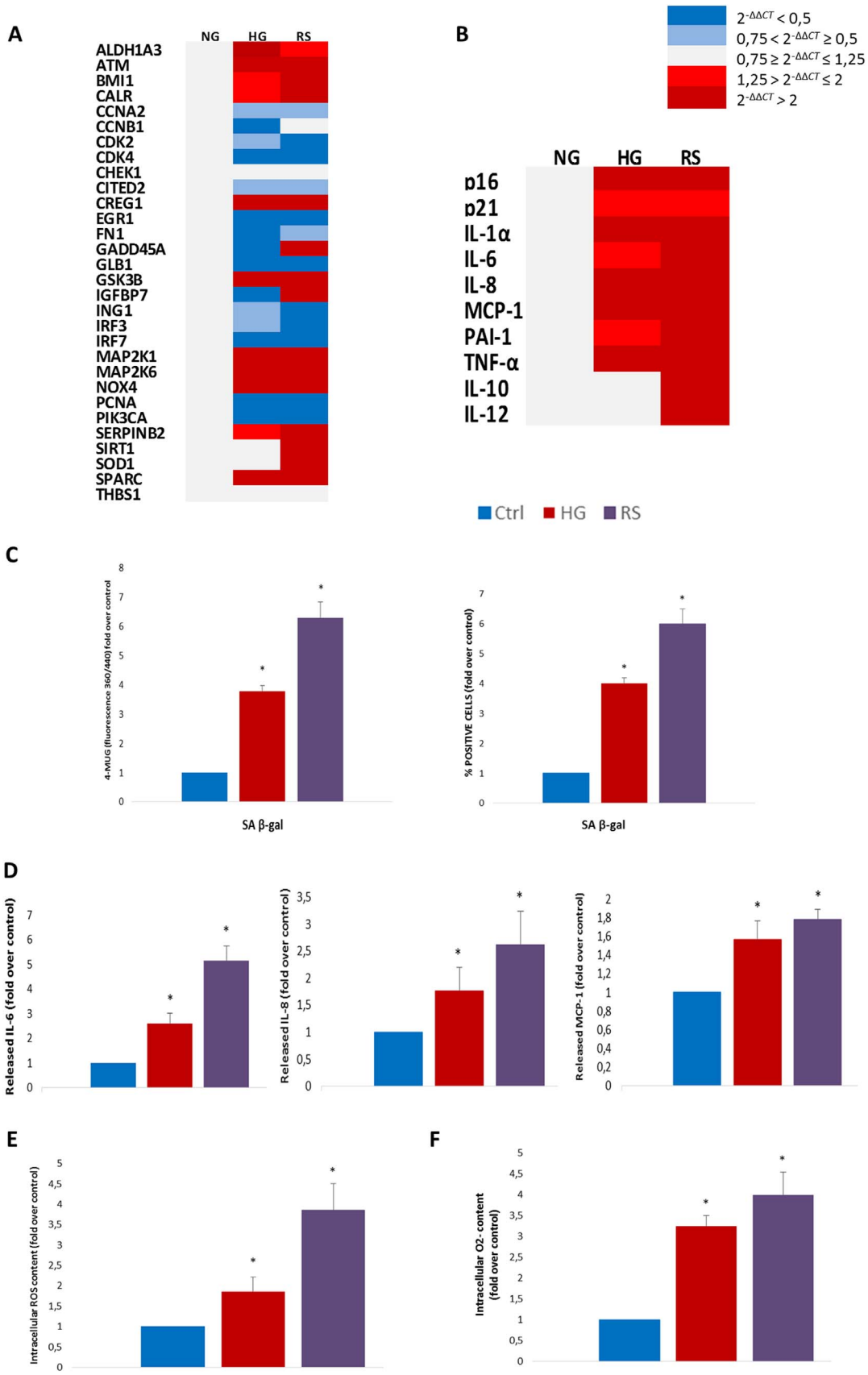

Fig. 3. Hyperglycaemia and replicative senescence trigger a comparable SASP in endothelial cells. HUVECs were exposed to 25 mM glucose for a week (HG), subcultured until replicative senescence (RS), or left untreated (Ctrl) A. Heatmap of SA mRNA array profiling. B. Heatmap of SASP mRNAs assessed by RT-PCR. $P < 0.05$ is intended for displayed mRNAs in HG and RS vs Ctrl. C. SA β-gal activity and percentage of SA β-gal + cells. D. IL-6, IL-8 and MCP-1 released in conditioned medium measured by ELISA. E. ROS assessment. F. O_2-. N = 3 for all experiments, consisting of 3 experiments with 3 different batches. Fold over control (arbitrary units) is intended for all diagrams. Blue histograms = means of control cells; red histograms = means of cells exposed to HG for a week; purple histograms = means of replicative senescent cells. For all diagrams error bars are ± SD and * *t*-test $p < 0.05$.

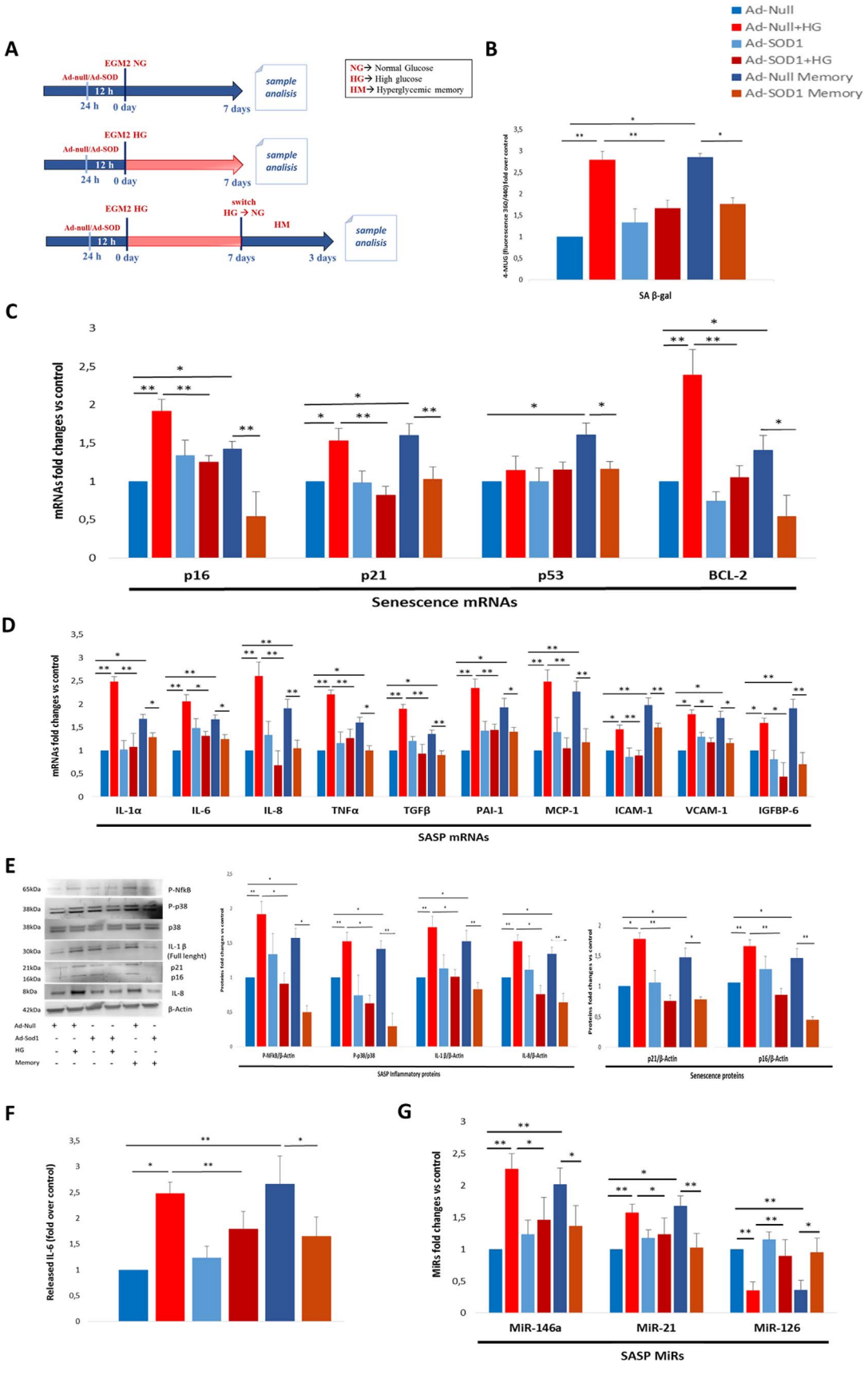

(caption on next page)

Fig. 4. Hyperglycaemia-induced senescence and SASP acquisition are prevented by SOD-1 overexpression in endothelial cells. A. Experimental design depicting normoglycaemic (NG), hyperglycaemic (HG) and hyperglycaemic memory (HM) treatments of HUVECs previously infected with adenovirus overexpressing SOD-1 (Ad-SOD-1) or GFP adenovirus (Ad-null) (both 10 MOI). B. SA β-gal activity. C. Fold changes in expression levels of SA mRNAs (*p16, p21, p53*, and *Bcl-2*). D. Fold changes in expression levels of SASP mRNAs (*IL-1α, IL-6, IL-8, TNF-α, TGF-β, PAI-1, MCP-1, ICAM-1*, *VCAM-1*, and *IGFBP6*). E. Western blot analysis of SA and SASP protein expression (p-NF-kB, p-p38, IL-1β, p21, p16, and IL-8). F. IL-6 released into culture medium, measured by ELISA. G. RT-PCR assessment of SASP-related miRNAs (*miR-146a, miR-21, and miR-126*). Fold over control (arbitrary units) is intended for all diagrams. Histograms show the means of cells treated as described (the treatment colour legend is reported in the figure). N = 4 (2 batches × 2 experiments) for all. For all diagrams error bars are ± SD and * *t*-test $p < 0.05$, ** *t*-test $p < 0.01$.

elevation in macrophages exposed to the hyperglycaemic medium (Fig. 5C). Accordingly, protein levels of procaspase-1, caspase-1, IL-1β, p-p38, and IL-8 were significantly increased in cells exposed to hyperglycaemic medium (Fig. 5D). However, since THP-1 cells are an immortalized cell line that does not express p16 in any of the conditions tested [35] (data not shown), a similar experiment was performed in U937-derived macrophages. HG exposure doubled SA β-gal positivity compared with control macrophages (Fig. 5E) and significantly increased both *p16* and *IL-6* expression (Fig. 5F), suggesting a phenotype consistent with the SASP. Finally, the mRNA expression of the genes characterizing M1/M2 was assessed to explore their modulation in the HG environment. The HG-triggered SASP in macrophages was characterized by a mixed phenotype with a predominance of M1, but some "non-M1" genes, specifically *TGF-β*, *MCP-1*, and *MMP-12*, were also significantly elevated [36] (Fig. 5C, G and Supplementary Table 3).

3.6. p16 and IL-8 mRNA transcripts are increased in circulating angiogenic cells from diabetic subjects

To gain preliminary information about the ability of the above-reported results to be extended to humans, blood samples were obtained from 13 type 2 diabetes patients and 10 age-matched healthy control subjects to isolate CACs from peripheral blood. CACs are endothelium/monocyte hybrid cells (CD34+/VEGFR2+) [37,38] that are selected by adherence to fibronectin-coated plates and play a recognized role in paracrine support to angiogenesis [38]. CACs from patients showed significantly increased *p16* and *IL-8* mRNA levels compared with those from control subjects (Fig. 6), suggesting a hyperglycaemic milieu veering towards the SASP also in *ex vivo* samples from diabetic patients.

4. Discussion

Obesity and diabetes are characterized by a subclinical, low-grade inflammation that is often denominated metaflammation. However, the mechanisms and cells fuelling this chronic state haven't been fully explored [1,2]. Recently, the SASP has been suggested to be a strong contributor to low-grade inflammation in both obesity and type 2 diabetes [3–8]. In several *in vivo* models accumulation of SCs and related inflammatory factors in fat tissue often precedes the loss of insulin sensitivity [12–14]. However, despite the large body of evidence for accelerated senescence that has been reported in the diabetic milieu [3,4,16,17], clear *in vivo* proof of SASP acquisition as a consequence of HG had not yet been provided. Here, we demonstrated that: i) an archetypal SASP response is induced in mouse kidney after one week of sustained, streptozotocin-induced HG, with endothelial cells and macrophages being SASP-carrying cells *in vivo*; ii) hyperglycaemic stimulus *in vitro* largely phenocopies the SASP acquired during replicative senescence in endothelial cell; iii) HG-induced senescence and SASP can be reverted by SOD-1 overexpression in endothelial cells; iiii) macrophages exposed to HG acquire features consistent with the SASP; and iiiii) *ex vivo* circulating angiogenic cells derived from peripheral blood mononuclear cells from diabetic patients displayed characteristics compatible with the SASP. Overall, the present findings support HG as a condition promoting the acquisition of SASP, making the SASP a highly likely contributor to the fuelling of low-grade inflammation in diabetes.

Regarding the first result, renal senescence has recently been described as a complex phenomenon in both physiological and pathological conditions [39,40]. In a mouse model of automated clearance, the renin-angiotensin-aldosterone system (RAAS) was among those most strongly affected by SC removal, indicating that SC accumulation in this organ may involve systemic consequences that go beyond low-grade inflammation [10,39]. The present work shows that one-week HG is sufficient to trigger senescence [39,41] and induce acquisition of a clear SASP. To the best of our knowledge, a fully-fledged SASP has never been described after short-term HG. This result lends support to the notion that HG can accelerate cellular ageing thus promoting the development of a low-grade inflammatory state [3,4]. Interestingly, β-gal positivity in cortical tubules was accompanied by a pro-senescence response in ECs and macrophages. Evidence of ECs senescence in the diabetic milieu has already been reported [15,16] as has sustained expression of pro-inflammatory genes following the hyperglycaemic insult [42]. Notably, HUVECs exposed to HG and those subcultured until growth arrest shared a closely overlapping transcriptional profile, but the former showed a blunted compensatory expression of the major anti-oxidant and anti-inflammatory genes SOD-1 and IL-10, a result that was also found in HG-exposed macrophages. Interestingly, diabetic subjects are characterized by reduced IL-10 secretion in response to whole blood LPS stimulation [43], whereas physiological ageing is associated with upregulation of this anti-inflammatory cytokine [44].

It has been suggested that HG-induced endothelial dysfunction may be driven by O_2- overproduction [29]. The present work provides data linking O_2- to senescence and the SASP, further supporting the well-established relationship between oxidative stress, ageing and low-grade inflammation [4]. According to a number of reports, some of the imbalances induced by HG are reversed in systems overexpressing SOD-1 [29,45]. Interestingly, the mitochondrial isoform SOD-2 has been shown to prevent skin senescence [46], with mitochondria-derived oxidative stress driving part the pro-inflammatory program of SCs [47]. A limitation of this study is that specific parameters of oxidative stress were not analysed, *e.g.* glutathione redox ratio. Nonetheless, the recent evidence that Sod1−/− mice exhibit increased renal senescence, SASP, and systemic low-grade inflammation corroborates the results presented here [48].

Macrophages bearing features consistent with the SASP are especially interesting, because they have recently been shown to determine the inflammatory microenvironment in the atherosclerotic plaque [18], together with senescent ECs and vascular smooth muscle cells [18,22]. The present work shows that HG can trigger the SASP in this cell type, suggesting a potential new contributor to the development of low-grade inflammation and possibly atherosclerosis, two pervasive features of type 2 diabetes [1–4]. Interestingly, as new senolytic and SASP-suppressing medications are developed, senescence and the SASP are fast becoming druggable targets [6,14,22,32,33,49]. The success of these drugs would be a major achievement, since current anti-inflammatory drugs have demonstrated a limited effect on diabetes progression or the development of its complications [50].

Diabetes is characterized by several factors that enhance the senescence burden, macrophage activation and a pro-inflammatory phenotype shift [2–4]. Different models of diabetic mice should be studied to gain a more thorough knowledge of these components before testing the hypothesis that long-term SCs removal or SASP attenuation could prolong the healthspan/lifespan of diabetic mice or slow diabetes progression and/or the development of its complications. However, the preliminary findings from our *ex vivo* experiment (CACs) indicate that the phenomena observed in the mouse models may be relevant to human diabetes [3,4,6–8,12].

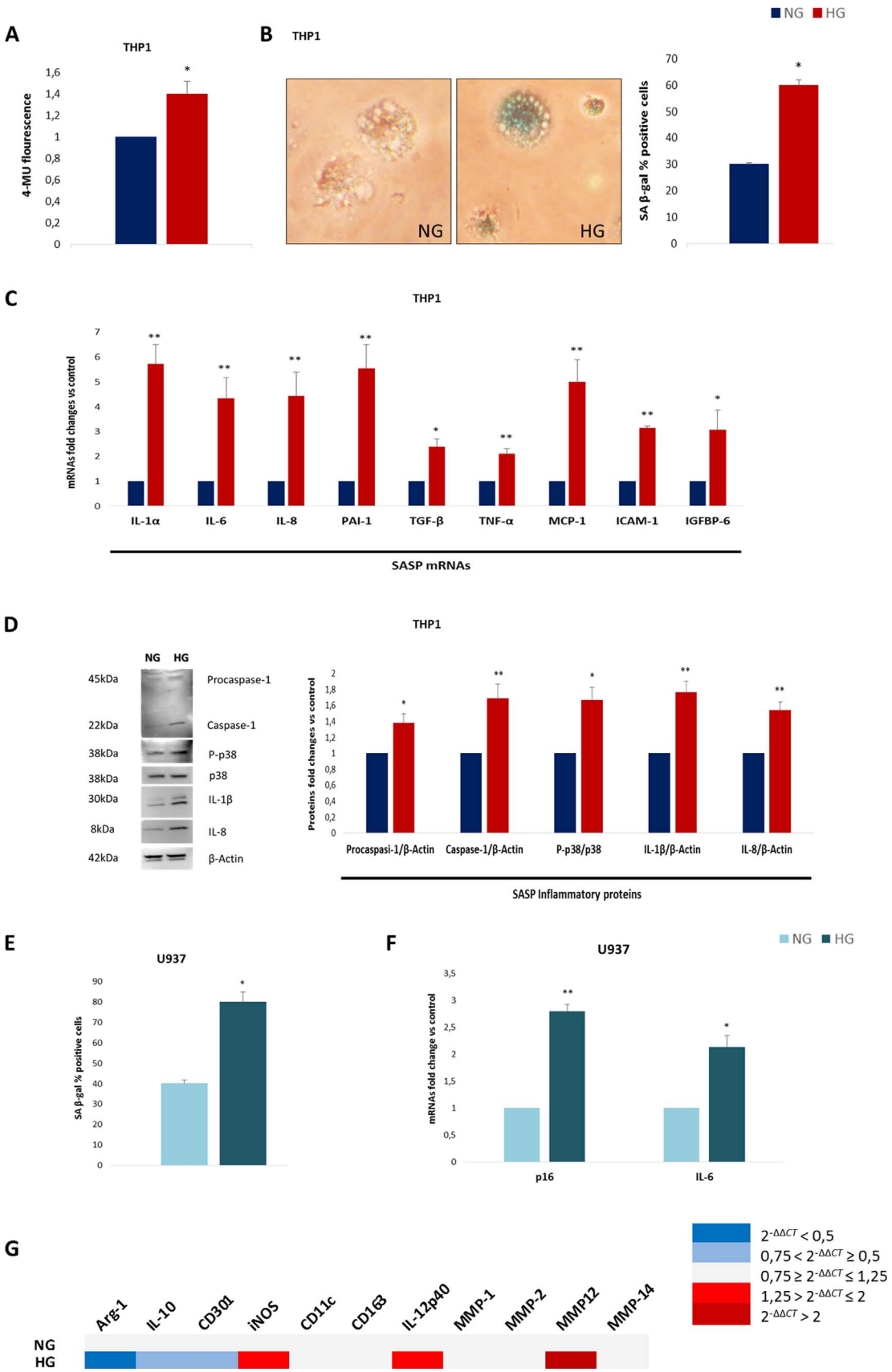

Fig. 5. Hyperglycaemia promotes a SASP-like program in cell line-derived macrophages. THP-1-derived macrophages were exposed to HG for a week. A. Measurement of SA β-gal activity. B. Representative images of SA β-gal staining (detail showing magnification of 40x images) with percentage of SA β-gal+ cells. C. Fold changes in expression levels of SASP mRNAs (*IL-1α, IL-6, IL-8, PAI-1, TGF-β, TNF-α, MCP-1, ICAM-1,* and *IGFBP6*). D. Western blot analysis of SASP proteins expression (procaspase-1, caspase-1, p-p38, IL-1β, and IL-8). The same experiment was performed in U937-derived macrophages. E. Percentage of SA β-gal+ cells. F. Fold changes in expression levels of *p16* and *IL-6* mRNAs. G. Heatmap of RT-PCR assessment of selected M1/M2 mRNAs in THP-1-derived macrophages. Histograms show the means of cells treated as described (the treatment colour legend is reported in the figure). N = 3 (experiments) for all. For all graphs error bars are ± SD and * *t*-test $p < 0.05$, ** *t*-test $p < 0.01$.

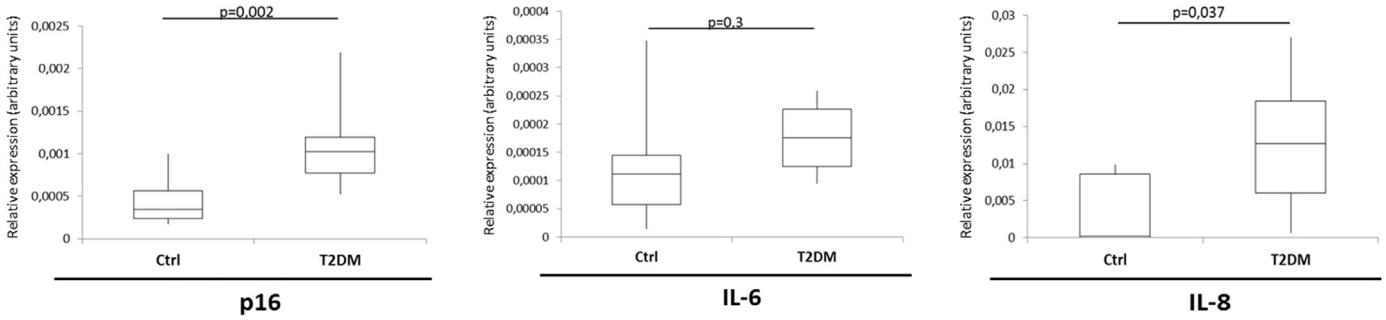

Fig. 6. Circulating angiogenic cells from diabetic patients show increased *p16* and *IL-8* mRNAs abundance. CACs were isolated from 13 type 2 diabetic patients and 10 age-matched control subjects. Boxplots show *p16*, *IL-6*, and *IL-8* mRNAs abundance for the two groups, with relative p values. P refers to two-tailed Student's *t*-test.

Altogether, the present findings indicate that the SASP is not only a possible cause of obesity-induced type 2 diabetes, but also a potential consequence of HG and point at a major role for ECs and macrophages as major SASP-carrying cells, thus adding a piece to the complex puzzle of metaflammation in diabetes.

Acknowledgements

We acknowledge Iñigo Chivite and Marc Claret from IDIBAPS for donating the mice organs. The authors are grateful to Word Designs for the language revision (www.silviamodena.com).

Author contributions

F.P., V.d.N., F.O. and A.C. designed the study. F.P., V.d.N., E.M., R.S., A.G, and G.M. performed the majority of experiments and analysed data. R.L. performed senescence mRNA profiling. R.R. and F.M. performed CACs purification and characterization. M.R.P., R.T., L.L.S., and A.D.P. revised the paper for intellectual content and provided additional expertise. F.P., E.M., and R.S. prepared figures and tables. F.P., F.O., and A.C wrote the paper. F.P takes responsibility for the contents of the article.

Sources of funding

This work was supported in part by grants from La Maratò de TV3 and from IDIBAPS to A.C.

Disclosures

None of the authors have competing interests.

Appendix A. Supplementary material

Supplementary data associated with this article can be found in the online version at http://dx.doi.org/10.1016/j.redox.2017.12.001.

References

[1] M.Y. Donath, S.E. Shoelson, Type 2 diabetes as an inflammatory disease, Nat. Rev. Immunol. 11 (2) (2011) 98–107.
[2] G.S. Hotamisligil, Inflammation, metaflammation and immunometabolic disorders, Nature 542 (7640) (2017) 177–185.
[3] A.K. Palmer, T. Tchkonia, N.K. LeBrasseur, E.N. Chini, M. Xu, J.L. Kirkland, Cellular senescence in type 2 diabetes: a therapeutic opportunity, Diabetes 64 (7) (2015) 2289–2298.
[4] F. Prattichizzo, V. De Nigris, L. La Sala, A.D. Procopio, F. Olivieri, A. Ceriello, "Inflammaging" as a druggable target: a senescence-associated secretory phenotype-centered view of type 2 diabetes, Oxid. Med. Cell Longev. 2016 1810327 (2016).
[5] C.D. Wiley, J. Campisi, From ancient pathways to aging cells-connecting metabolism and cellular senescence, Cell Metab. 14 (6) (2016) 1013–1021 (23).
[6] A.K. Palmer, J.L. Kirkland, Aging and adipose tissue: potential interventions for diabetes and regenerative medicine, Exp. Gerontol. 15 (86) (2016) 97–105.
[7] M.J. Schafer, T.A. White, G. Evans, et al., Exercise prevents diet-induced cellular senescence in adipose tissue, Diabetes 65 (6) (2016) 1606–1615.
[8] A. Villaret, J. Galitzky, P. Decaunes, D. Estève, M.A. Marques, C. Sengenès, P. Chiotasso, T. Tchkonia, M. Lafontan, J.L. Kirkland, A. Bouloumié, Adipose tissue endothelial cells from obese human subjects: differences among depots in angiogenic, metabolic, and inflammatory gene expression and cellular senescence, Diabetes 59 (11) (2010) 2755–2763.
[9] J.P. Coppé, P.Y. Desprez, A. Krtolica, J. Campisi, The senescence-associated secretory phenotype: the dark side of tumor suppression, Annu. Rev. Pathol. 5 (2010) 99–118.
[10] D.J. Baker, B.G. Childs, M. Durik, M.E. Wijers, C.J. Sieben, J. Zhong, R.A. Saltness, K.B. Jeganathan, G.C. Verzosa, A. Pezeshki, K. Khazaie, J.D. Miller, J.M. van Deursen, Naturally occurringp16(Ink4a)-positive cells shorten healthy lifespan, Nature 530 (7589) (2016) (184-p19).
[11] C. Franceschi, M. Bonafè, S. Valensin, F. Olivieri, M. De Luca, E. Ottaviani, G. De Benedictis, Inflamm-aging. An evolutionary perspective on immunosenescence, Ann. N. Y. Acad. Sci. 908 (2000) 244–254.
[12] T. Minamino, M. Orimo, I. Shimizu, T. Kunieda, M. Yokoyama, T. Ito, A. Nojima, A. Nabetani, Y. Oike, H. Matsubara, F. Ishikawa, I. Komuro, A crucial role for adipose tissue p53 in the regulation of insulin resistance, Nat. Med. 15 (9) (2009) 1082–1087.
[13] I. Shimizu, Y. Yoshida, T. Katsuno, K. Tateno, S. Okada, J. Moriya, M. Yokoyama, A. Nojima, T. Ito, R. Zechner, I. Komuro, Y. Kobayashi, T. Minamino, p53-induced adipose tissue inflammation is critically involved in the development of insulin resistance in heart failure, Cell Metab. 15 (1) (2012) 51–64.
[14] M. Xu, A.K. Palmer, H. Ding, M.M. Weivoda, T. Pirtskhalava, T.A. White, A. Sepe, K.O. Johnson, M.B. Stout, N. Giorgadze, M.D. Jensen, N.K. LeBrasseur, T. Tchkonia, J.L. Kirkland, Targeting senescent cells enhances adipogenesis and metabolic function in old age, Elife 4 (2015) e12997.
[15] Y. Li, Tollefsbol TO. p16(INK4a) suppression by glucose restriction contributes to human cellular lifespan extension through SIRT1-mediated epigenetic and genetic mechanisms, PLoS One 6 (2) (2011) e17421, http://dx.doi.org/10.1371/journal.pone.0017421.
[16] J. Chen, S.V. Brodsky, D.M. Goligorsky, D.J. Hampel, H. Li, S.S. Gross, M.S. Goligorsky, Glycated collagen I induces premature senescence-like phenotypic changes in endothelial cells, Circ. Res. 90 (12) (2002) 1290–1298.
[17] D. Verzola, M.T. Gandolfo, G. Gaetani, A. Ferraris, R. Mangerini, F. Ferrario, B. Villaggio, F. Gianiorio, F. Tosetti, U. Weiss, P. Traverso, M. Mji, G. Deferrari, G. Garibotto, Accelerated senescence in the kidneys of patients with type 2 diabetic nephropathy, Am. J. Physiol. Ren. Physiol. 295 (5) (2008) F1563–F1573.
[18] B.G. Childs, D.J. Baker, T. Wijshake, C.A. Conover, J. Campisi, J.M. van Deursen, Senescent intimal foam cells are deleterious at all stages of atherosclerosis, Science 354 (6311) (2016) 472–477.
[19] B.M. Hall, V. Balan, A.S. Gleiberman, E. Strom, P. Krasnov, L.P. Virtuoso, E. Rydkina, S. Vujcic, K. Balan, I. Gitlin, K. Leonova, A. Polinsky, O.B. Chernova, A.V. Gudkov, Aging of mice is associated with p16(Ink4a)- and β-galactosidase-positive macrophage accumulation that can be induced in young mice by senescent cells, Aging 8 (7) (2016) 1294–1315.
[20] G.H. Tesch, T.J. Allen, Rodent models of streptozotocin-induced diabetic nephropathy, Nephrology 12 (3) (2007) 261–266.
[21] G.P. Dimri, X. Lee, G. Basile, M. Acosta, G. Scott, C. Roskelley, E.E. Medrano, M. Linskens, I. Rubelj, O. Pereira-Smith, A biomarker that identifies senescent human cells in culture and in aging skin in vivo, Proc. Natl. Acad. Sci. USA 92 (20) (1995) 9363–9367.
[22] S.E. Gardner, M. Humphry, M.R. Bennett, M.C. Clarke, Senescent vascular smooth muscle cells drive inflammation through an interleukin-1α-dependent senescence-associated secretory phenotype, Arterioscler. Thromb. Vasc. Biol. 35 (9) (2015) 1963–1974.
[23] E. Schraml, J. Grillari, From cellular senescence to age-associated diseases: the miRNA connection, Longev. Health Span 1 (1) (2012) 10.
[24] F. Prattichizzo, A. Giuliani, V. De Nigris, G. Pujadas, A. Ceka, L. La Sala, S. Genovese, R. Testa, A.D. Procopio, F. Olivieri, A. Ceriello, Extracellular microRNAs and endothelial hyperglycaemic memory: a therapeutic opportunity? Diabetes Obes. Metab. 18 (9) (2016) 855–867.
[25] M. Kölling, T. Kaucsar, C. Schauerte, et al., Therapeutic miR-21 silencing ameliorates diabetic kidney disease in mice, Mol. Ther. 4 (1) (2017) 165–180 (25).
[26] K. Bhatt, L.L. Lanting, Y. Jia, S. Yadav, M.A. Reddy, N. Magilnick, M. Boldin, R. Natarajan, Anti-inflammatory role of MicroRNA-146a in the pathogenesis of

diabetic nephropathy, J. Am. Soc. Nephrol. 27 (8) (2016) 2277–2288.
[27] J.C. Acosta, A. Banito, T. Wuestefeld, et al., A complex secretory program orchestrated by the inflammasome controls paracrine senescence, Nat. Cell Biol. 15 (8) (2013) 978–990.
[28] A. Freund, C.K. Patil, J. Campisi, p38MAPK is a novel DNA damage response-independent regulator of the senescence-associated secretory phenotype, EMBO J. 30 (8) (2011) 1536–1548.
[29] A. Ceriello, E. Motz, Is oxidative stress the pathogenic mechanism underlying insulin resistance, diabetes, and cardiovascular disease? The common soil hypothesis revisited, Arterioscler. Thromb. Vasc. Biol. 24 (5) (2004) 816–823 (Epub 2004 Feb 19. Review).
[30] B. Lener, R. Kozieł, H. Pircher, E. Hütter, R. Greussing, D. Herndler-Brandstetter, M. Hermann, H. Unterluggauer, P. Jansen-Dürr, The NADPH oxidase Nox4 restricts the replicative lifespan of human endothelial cells, Biochem. J. 423 (3) (2009) 363–374.
[31] D. Koya, G.L. King, Protein kinase C activation and the development of diabetic complications, Diabetes 47 (6) (1998) 859–866 (Review).
[32] Y. Zhu, T. Tchkonia, H. Fuhrmann-Stroissnigg, H.M. Dai, Y.Y. Ling, M.B. Stout, T. Pirtskhalava, N. Giorgadze, K.O. Johnson, C.B. Giles, J.D. Wren, L.J. Niedernhofer, P.D. Robbins, J.L. Kirkland, Identification of a novel senolytic agent, navitoclax, targeting the Bcl-2 family of anti-apoptotic factors, Aging Cell 15 (3) (2016) 428–435.
[33] R. Yosef, N. Pilpel, R. Tokarsky-Amiel, A. Biran, Y. Ovadya, S. Cohen, E. Vadai, L. Dassa, E. Shahar, R. Condiotti, I. Ben-Porath, V. Krizhanovsky, Directed elimination of senescent cells by inhibition of BCL-W and BCL-XL, Nat. Commun. 7 (2016) 11190.
[34] E.K. Park, H.S. Jung, H.I. Yang, M.C. Yoo, C. Kim, K.S. Kim, Optimized THP-1 differentiation is required for the detection of responses to weak stimuli, Inflamm. Res. 56 (1) (2007) 45–50.
[35] Y. Murakami, F. Mizoguchi, T. Saito, N. Miyasaka, H. Kohsaka, p16(INK4a) exerts an anti-inflammatory effect through accelerated IRAK1 degradation in macrophages, J. Immunol. 189 (10) (2012) 5066–5072.
[36] F.O. Martinez, S. Gordon, M. Locati, A. Mantovani, Transcriptional profiling of the human monocyte-to-macrophage differentiation and polarization: new molecules and patterns of gene expression, J. Immunol. 177 (10) (2006) 7303–7311.
[37] F. Olivieri, R. Antonicelli, R. Recchioni, S. Mariotti, F. Marcheselli, R. Lisa, L. Spazzafumo, R. Galeazzi, D. Caraceni, R. Testa, R. Latini, A.D. Procopio, Telomere/telomerase system impairment in circulating angiogenic cells of geriatric patients with heart failure, Int. J. Cardiol. 164 (1) (2013) 99–105.
[38] J. Rehman, J. Li, C.M. Orschell, K.L. March, Peripheral blood "endothelial progenitor cells" are derived from monocyte/macrophages and secrete angiogenic growth factors, Circulation 107 (2003) 1164–1169.
[39] I. Sturmlechner, M. Durik, C.J. Sieben, D.J. Baker, J.M. van Deursen, Cellular senescence in renal ageing and disease, Nat. Rev. Nephrol. 13 (2) (2017) 77–89.
[40] W.J. Wang, G.Y. Cai, X.M. Chen, Cellular senescence, senescence-associated secretory phenotype, and chronic kidney disease, Oncotarget (2017) (Epub ahead of print) (Review).
[41] J. Satriano, H. de Mansoury, A. Deng, K. Sharma, V. Vallon, R.C. Blantz, S.C. Thomson, Transition of kidney tubule cells to a senescent phenotype in early experimental diabetes, Am. J. Physiol. Cell Physiol. 299 (2) (2010) C374–C380.
[42] L. Pirola, A. Balcerczyk, R.W. Tothill, et al., Genome-wide analysis distinguishes hyperglycemia regulated epigenetic signatures of primary vascular cells, Genome Res. 21 (10) (2011) 1601–1615.
[43] E. Van Exel, J. Gussekloo, A.J. de Craen, M. Frölich, A. Bootsma-Van Der Wiel, R.G. Westendorp, Leiden 85 Plus Study, Low production capacity of interleukin-10 associates with the metabolic syndrome and type 2 diabetes: the Leiden 85-Plus Study, Diabetes 51 (4) (2002) 1088–1092.
[44] I.M. Rea, O.A. Ross, M. Armstrong, S. McNerlan, D.H. Alexander, M.D. Curran, D. Middleton, Interleukin-6-gene C/G 174 polymorphism in nonagenarian and octogenarian subjects in the BELFAST study. Reciprocal effects on IL-6, soluble IL-6 receptor and for IL-10 in serum and monocyte supernatants, Mech. Ageing Dev. 124 (4) (2003) 555–561.
[45] M. Zanetti, J. Sato, Z.S. Katusic, T. O'Brien, Gene transfer of superoxide dismutase isoforms reverses endothelial dysfunction in diabetic rabbit aorta, Am. J. Physiol. Heart Circ. Physiol. 280 (6) (2001) H2516–H2523.
[46] M.C. Velarde, J.M. Flynn, N.U. Day, S. Melov, J. Campisi, Mitochondrial oxidative stress caused by Sod2 deficiency promotes cellular senescence and aging phenotypes in the skin, Aging 4 (1) (2012) 3–12.
[47] V.I. Korolchuk, S. Miwa, B. Carroll, T. von Zglinicki, Mitochondria in cell senescence: is mitophagy the weakest link? EBioMed. S2352–3964 (17) (2017) (30116-0).
[48] Y. Zhang, A. Unnikrishnan, S.S. Deepa, Y. Liu, Y. Li, Y. Ikeno, D. Sosnowska, H. Van Remmen, A. Richardson, A new role for oxidative stress in aging: the accelerated aging phenotype in Sod1$^{-/-}$ mice is correlated to increased cellular senescence, Redox Biol. 11 (2017) 30–37, http://dx.doi.org/10.1016/j.redox.2016.10.014 (Epub 2016 Nov 2).
[49] J.L. Kirkland, T. Tchkonia, Cellular senescence: a translational perspective, EBioMed. S2352–3964 (17) (2017) 30154–30158 (Review).
[50] R.M. Pollack, M.Y. Donath, D. LeRoith, G. Leibowitz, Anti-inflammatory agents in the treatment of diabetes and its vascular complications, Diabetes Care 2 (2016) S244–S252.
[51] F. Prattichizzo, A. Giuliani, R. Recchioni, M. Bonafè, F. Marcheselli, S. De Carolis, A. Campanati, K. Giuliodori, M.R. Rippo, F. Brugè, L. Tiano, C. Micucci, A. Ceriello, A. Offidani, A.D. Procopio, F. Olivieri, Anti-TNF-α treatment modulates SASP and SASP-related microRNAs in endothelial cells and in circulating angiogenic cells, Oncotarget 7 (11) (2016) 11945–11958.
[52] C. Mas-Bargues, J. Viña-Almunia, M. Inglés, J. Sanz-Ros, J. Gambini, J.S. Ibáñez-Cabellos, J.L. García-Giménez, J. Viña, C. Borrás, Role of p16INK4a and BMI-1 in oxidative stress-induced premature senescence in human dental pulp stem cells, Redox Biol. 12 (2017) 690–698, http://dx.doi.org/10.1016/j.redox.2017.04.002 (Epub 2017 Apr 7).